44. Jahrestagung für Akustik (DAGA 2018), München

Sensors for the Measurement of Flow Induced Surface Pressure Fluctuations: Calibration and Detection of Clipping

Farhan Ahmed Manegar[1], Kathrin Stahl[2], Thomas Carolus[3]

[1] *University of Siegen, 57068 Siegen, E-Mail: farhan.manegar@uni-siegen.de*
[2] *University of Siegen, 57068 Siegen, E-Mail: kathrin.stahl@uni-siegen.de*
[3] *University of Siegen, 57068 Siegen, E-Mail: thomas.carolus@uni-siegen.de*

Abstract

Flow induced surface pressure fluctuations are thought to be the elementary sources of sound emitted from bodies subjected to a flow. In many direct high fidelity computational aeroacoustic simulations, the surface pressure fluctuations are obtained as an intermediate result and serve as an input for determining the acoustic field. It is therefore of utmost interest to reliably measure these quantities. The paper presents a study of how to select and calibrate sensors for the measurement of surface pressure fluctuations. Calibration methods are compiled and compared. A method for detecting clipping due to overload of a sensor is presented. Eventually, in an in-house built experimental setup, different tests of two types of miniature electret condenser microphones, flush-mounted in the trailing edge region of a wind turbine blade section, are carried out.

Description of problem and objectives

Flow induced surface pressure fluctuations are thought to be the elementary sources of sound emitted from bodies subjected to a flow. In many direct high fidelity computational aeroacoustic simulations, the surface pressure fluctuations are obtained as an intermediate result and serve as an input for determining the acoustic field. It is therefore of utmost interest to reliably measure these quantities as well. For many years various miniature transducers, either mounted beneath a pin hole on the surface or connected to pin hole with a capillary tube or just flush mounted have been used on stationary airfoils sections and rotating turbo machinery blades. In recent years frequently miniature electret microphones became increasingly popular – for several reasons: They are very small, do not need external signal amplification and are low-cost. **Fig. 1** shows miniature microphones flush mounted on a fan blade and in-situ calibration with pre-calibrated headphones.

For reliable measurements, however two key issues have to be addressed: (i) selection of the sensor with respect to sensitivity and (ii) its calibration.

Objectives of this contribution are: (i) a comparison of the "acoustic" with the "hydrodynamic" calibration (the term "hydrodynamic" refers to the idea of using pressure fluctuations generated by a turbulent flow over a surface instead of acoustic waves as a calibration signal), (ii) a method for detecting clipping of a signal which unexpectedly might occur when "misusing" microphones for measuring flow induced surface pressure fluctuations.

Sensor tested and test setup

The study deals with the sensors from Tab. 1 and shown in

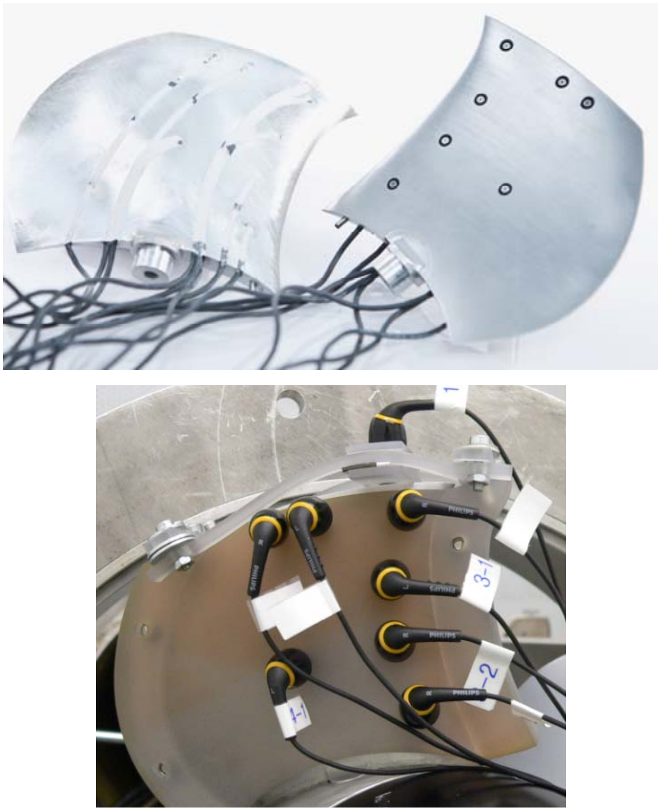

Fig. 1: Miniature microphones on a fan blade (top) and in-situ calibration with pre-calibrated headphones on a clamp-on adapter (bottom), from [1]

Fig. 2. Sensor a is an expensive probe microphone. Originally it was designed for sound pressure measurements in small or awkward places or in harsh environments where a conventional microphone would be unsuitable. The probe microphone has a smooth frequency response from 1 Hz to 20 kHz, with a very smooth high-frequency roll-off. The dynamic range is 42 - 164 dB. An important feature of a is its internal tube which is used to match the impedance at the exit of the tiny cavity in front of the microphone diaphragm. This significantly reduces the effects of reflections within the probe tube. In this study a serves as the reference sensor for the pressure fluctuations of interest. Prior to any measurements, it is calibrated via a Brüel & Kjær pistonphone type 4231 to which the probe microphone is connected via an adapter. Sensors b and c are standard

miniature electret microphones. They are candidates for instrumentation of a section of a wind turbine blade for aerodynamic testing.

Tab. 1 Sensors employed within this study

	Description	Brand and type	Effective diameter [mm]	Sensing diameter [mm]	Nominal sensitivity [mV/Pa]	Dynamic range [dB]
a	Probe microphone (1/4″ condenser microphone with a 50 mm long probe tube) with Nexus amplifier	Brüel & Kjær 4182	1.24	(1/4″ condenser microphone)	3.16	42 to 164 dB
b	Miniature electret microphone	Knowles FG 45 32335 P03	2.57	0.76	436.52	till 150 dB
c	Miniature electret microphone	Knowles FG 23229 P07	2.57	0.76	543.25	till 118 dB

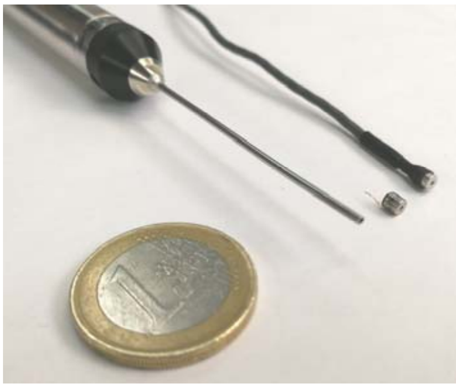

Fig. 2: Sensors in this study: Sensor *a*, sensor *b* and sensor *c* (from left to right)

p(t) is the pressure a function of time. The power spectral density (PSD)

$$S_{pp}(f) = \lim_{\Delta f \to 0} \frac{p^2(f)}{\Delta f} \qquad [\mathrm{Pa^2/Hz}], \tag{1}$$

can be interpreted as the averaged power of the pressure fluctuation at each frequency in an infinitesimally small frequency band Δf. The quantity considered is the power spectral density *level* (PSDL) of the pressure fluctuation which is formulated as

$$L_{spp}(f) = 10\log\left(\frac{S_{pp}(f)\cdot\Delta f_{ref}}{p_{ref}^2}\right) \quad \mathrm{dB} \tag{2}$$

with a reference frequency band Δf_{ref} = 1 Hz and a reference pressure $p_{ref} = 2\cdot10^{-5}$ Pa. In practice, $S_{pp}(f)$ is calculated by a Fast-FOURIER transform of the autocorrelation function $R_{pp}(\tau)$

$$S_{pp}(f) = \int_{-\infty}^{\infty} R_{pp}(\tau) e^{-i\cdot 2\cdot\pi\cdot f\cdot\tau} d\tau \tag{3}$$

where i is the imaginary unit and τ is the time delay, given the autocorrelation function

$$R_{pp}(\tau) = \lim_{t_1\to\infty} \frac{1}{t_1} \int_0^{t_1} p(t)\cdot p(t+\tau)\, dt \tag{4}$$

of the pressure fluctuation *p(t)*. With the overall power in a frequency range from f_1 to f_2

$$P_{p,overall} = \sum_{f_1}^{f_2} S_{pp}(f)\cdot\Delta f \tag{5}$$

the overall power spectrum level $L_{p,overall}$ is then given as

$$L_{p,overall} = 10\,log\left(\frac{P_{p,overall}}{p_{ref}^2}\right) \tag{6}$$

Throughout this paper all time signals were captured by a 16 a channel 24-bit NATIONAL INSTRUMENTS® data acquisition card (model type PXI-4495) with a sampling rate f_s = 51200 Hz for a time period of 30 s. Equation (1) is evaluated by the function *pwelch* in MATLAB® Version R2016b. The parameters chosen for *pwelch* are window = hann, noverlap = 0.5. The spectra from the windows have been averaged. For all levels, the reference pressure is p_{ref} = 2x10^{-5} Pa. If not specified otherwise, this study uses the standard frequency resolution Δf_{res} = 10 Hz and an overall level of the sound pressure in the range of f_1 = 100 Hz and f_2 = 10.000 Hz.
Three different set-ups for the experiments have been given. For all variations the sensors were placed close to the trailing edge of the airfoil. Individuals of each type of sensor *b* and *c* are flush mounted in a comparably small region close to the trailing edge of an airfoil section, see **Fig. 3**. The opening of the tube from the probe microphone *a* is placed close to the sensors. In set-up I the flow induced surface pressure fluctuation were taken as test signal. The bulky part of the probe microphone *a* sits below the airfoil, with the tube sticking through a hole in the same chordwise position as the sensors. It is worth to note that the size of the probe tube and the pin hole openings of the sensors *b* and *c* is similar. For test set-up II the reference sound source Brüel & Kjær Type 4204 (de facto a centrifugal fan) emitting a broad band sound was used, for set-up III a headphone (Sennheiser HD 650) with a broadband electric signal.

Results

A. Detection of clipping

Clipping occurs when the input signal to a sensor has achieved the maximum of its dynamic range. It is undesired, since it distorts the measured signal. The sensors were tested in test set-up I with the flow induced signal (see **Fig. 3a**). The PSDL of the sensor *a*, *b* and *c* are shown in **Fig. 4**. Initially, the sensitivity of sensor *c* as specified by the manufacturer for purely acoustic signals was considered to be suitable for the expected hydrodynamic pressure fluctuations, i.e. no clipping was expected. However, the signal from sensor type *c* did not show the expected trend, i.e. an increase in the amplitudes of flow induced surface pressure fluctuations with an increase of free field flow velo city u_∞.

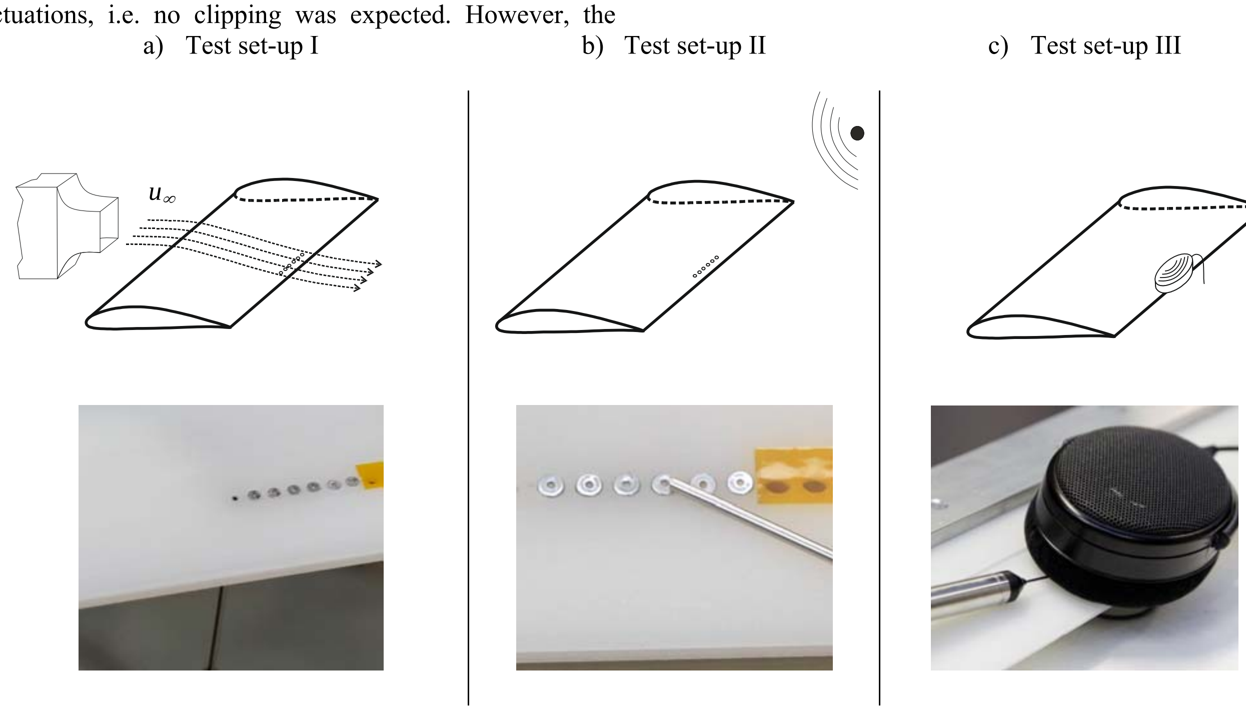

Fig. 3 Test set ups: a) hydrodynamic b) acoustic signal from free field sound source, c) acoustic signal from headphone

This gave rise to the question how clipping can be detected. In Aleinik et al. [2] and Laguna et al. [3] an amplitude histogram is employed to detect clipping for speech signals. The distribution density of the amplitudes of non-clipped signals yields symmetric distributions similar to Laplace or Gaussian distributions. If clipping occurs, sharp bursts on the left and right tail ends appear, caused by the concentration of samples at the threshold of the dynamic range of the sensors. **Fig. 5** shows the time traces of the raw signals and their amplitude histograms. From top to bottom the flow velocity and hence the strength of the pressure fluctuations are increased. An unclipped signal, e.g. for u_∞ = 16 m/s, clearly shows a Gaussian distribution. At u_∞ = 23 m/s, the time signal does not look clipped. However, if we look into the corresponding histogram, little bursts appear on the left and right tail of the histogram. By increasing the velocity further, the bursts continue to grow and the time signals are clearly clipped.

C. Effect of the type of calibration on calibration curves

To have a fair comparison of the calibration curves from three different set-ups, we aimed at a similar source strength of the test signals. In set-up I (hydrodynamic) and set-up III (acoustic), the $L_{p,\,overall}$ was 94 dB, however, for set-up II, the available source in free field only produced $L_{p,\,overall}$ = 65 dB as a test signal.

Acoustical calibration is carried out by placing the opening of the tube from the probe microphone *a* 1 mm above each sensor (see **Fig. 3b** and **3c**). A broadband sound field without any flow is used as sound source. Two set-ups for acoustical calibration were applied: Set-up II with a sound generating device in the free field (Fig. **3b**) and set-up III with a headphone located very close to the sensors (Fig. **3c**). A similar set-up has been described in van der Velden et al. [4] and Bilka et al. [5]. In case of hydrodynamic calibration

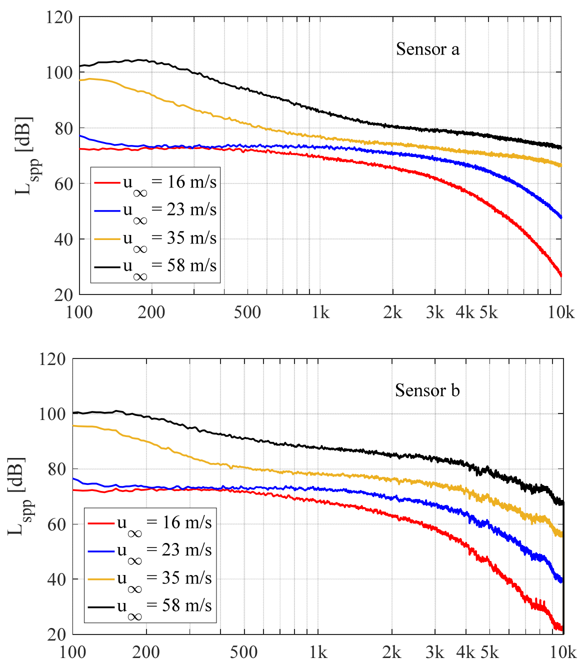

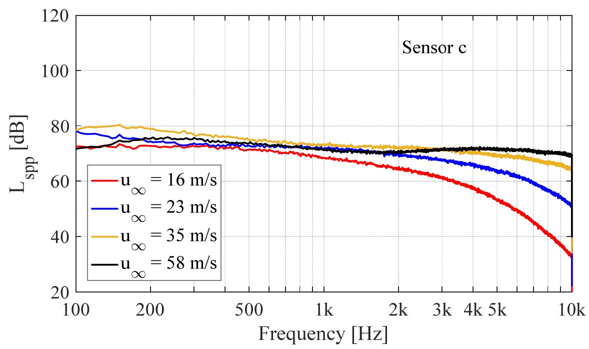

Fig. 4 *PSDL* of hydrodynamic pressure fluctuations obtained with sensor *a,b* and *c*; sensor *c* is not suitable for the level of the test signals applied.

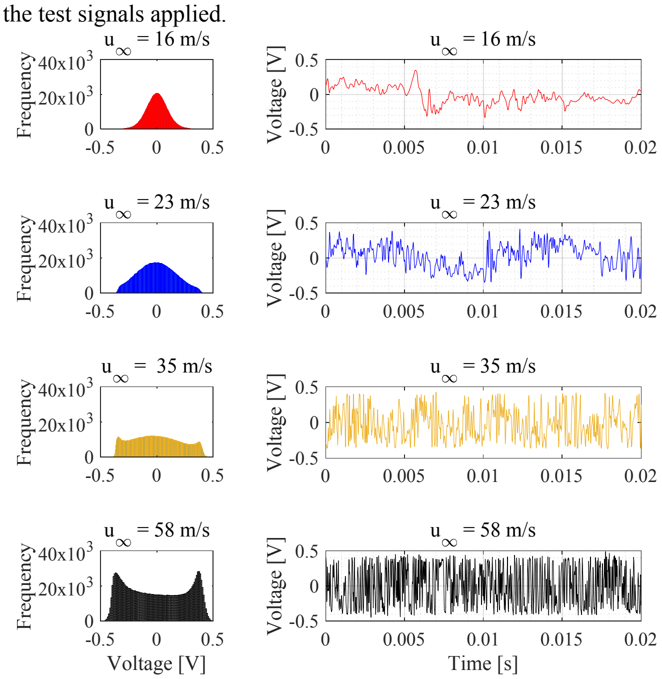

Fig. 5 Time traces and amplitude histograms of the raw signal from sensor *c* for increasing flow velocity; clipping is clearly visible for $u_\infty \geq 35$ m/s.

the complete assembly is placed in a low noise aeroacoustic wind tunnel providing a low noise jet of variable flow velocity u_∞ up to some 60 m/s. The hydrodynamic pressure fluctuations due to the turbulent boundary layer above the sensors serve as test signals and are assumed to be seen by all sensors equally (**Fig. 3a**). The simultaneous capturing of the signals eventually allows establishing a frequency-dependent calibration factor *C* for sensors *b* and *c* with respect to the reference sensor *a*:

$$C(f) = 10 \log \left(\frac{S_{pp\,Sensor\,a}(f)}{S_{pp\,Sensor\,(b\,or\,c)}(f)} \right) \quad \text{dB} \qquad (7)$$

Fig. 6 shows three calibration curves for the sensor type *b* with respect to the probe microphone sensor *a*. In a frequency range between 150 Hz to 1 kHz, calibration from set-up I and II yield very similar calibration factors *C* with a deviation of 1 dB at 1 kHz. At higher frequencies the mismatch rises up to 5 dB. The comparison of acoustic calibration curve realised with set-up III (head phones) to the hydrodynamic curve (set-up I) shows good agreement between 500 Hz and 4 kHz. For lower and higher frequencies there are variations up to 8 dB.

Conclusion

As a conclusion the miniature microphones investigated respond to pressure fluctuations regardless of whether the fluctuations come from acoustic or hydrodynamic sources. Detection of clipping is essential when investigating flow induced pressure fluctuations, since it affect the quality of the signal. To detect clipping the amplitude histogram of the time signal can be employed as a useful tool. However, detection of clipping should be employed in every post processing whereas measuring acoustic or hydrodynamic signals.

Once clipping is ruled out, all calibration methods, hydrodynamic and acoustic, can be employed. The easy and fast acoustic calibration (set-up III), however, has deviations at lower and higher frequencies. If signals with low and/or high frequency components are to be investigated, a hydrodynamic calibration seems to be indispensable.

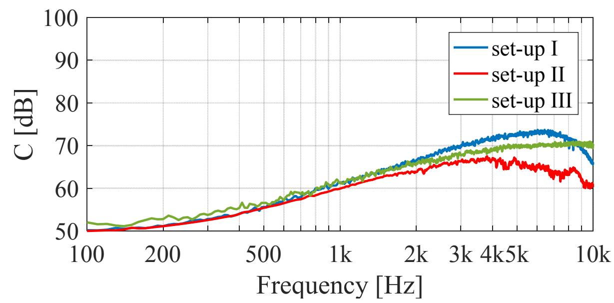

Fig. 6 Calibration curves of a sensor type *b* obtained via hydrodynamic (set-up I) and acoustic calibration (set-up II & III) with respect to probe microphone sensor *a*

References

[1] Zhu, T., Lallier-Daniels, D., Sanjosé, M., Moreau, S., Carolus, T., **2016**, "Rotating Coherent Flow Structures as a Source for Narrowband Tip Clearance Noise from Axial Fan", 22nd AIAA/CEAS Aeroacoustics Conference, 30.5. - 1.6.2016, Lyon, France

[2] Aleinik, S., Matveev, Y., **2014**, "Detection of Clipped Fragments in Speech Signals. International Journal of Computer and Information Engineering", Vol. 8, No. 2

[3] Laguna, C., Lerch, A., **2016**, "An Efficient Algorithm for Clipping Detection and Declipping Audio", 141st Convention Audio Engineering Society, 02.10.2016, Los Angeles, USA

[4] van der Velden, W.C.P., Pröbsting, S., Zuijlen, A.H., de Jong, A.T., Guan, Y., Morris, S.C., **2016**, "Numerical and experimental investigation of a bevelled trailing-edge flow field and noise emission. Journal of Sound and Vibration", 384, pp 113-129

[5] Bilka, M., Morris, S.C., Berntsen, C., Silver, J.C., Shannon, D.W., **2014**, "Flow field and sound from a blunt trailing edge with varied thickness", AIAA Journal, 52, pp 52-61